SHEATH PROPERTIES AND RELATED PHENOMENA OF THE PLASMA WALL INTERACTION IN MAGNETISED PLASMAS. APPLICATION TO ITER

G. Popa, Steluța Teodoru, C. Costin, C. Lupu

"Al. I. Cuza" University, Faculty of Physics, Iasi

1. Introduction

Physics of the sheath formed between the plasma and the solid electrodes and/or the walls is still one of the most important and complicated problems of plasma physics and technology. It is even more complicated in the case of magnetised hot plasmas due to the high magnetic field strengths and the large particle flux densities towards the walls, limiters and divertor plate of the TOKAMAK devices. Both the edge plasma and the ion sheath resulting from the interaction of the particles with the surfaces play an important role in the absorption of energy and radiation and in the overall energy balance in the machine as JET and ITER. Therefore it is important to analyse the composition and the properties of the edge plasma.

The purpose of the present work was to use experience and collaborations of the plasma group of the "Al. I. Cuza" University in treatment of the plasma-wall transition problem in front of an electrode or the chamber wall both theoretically and experimentally. The theoretical approach comprises fluid theory, kinetic theory and numerical simulations.

In the field of numerical simulations applied to fluid theory, a 2D time-dependent fluid model was considered to be applied for hydrogen plasma. In spite of the fact that there exists a large amount of knowledge on the plasma-wall transition problem, the related fluid boundary conditions for the energy and momentum equations are not complete. This problem is even more difficult in the case of multi-fluid plasmas with strong drifts and currents and/or strong wall effects (such as secondary-electron emission).

Moreover, kinetic modelling of the collisionless region was considered as a rather complex problem, even for the idealised case of a two-species plasma (electron-ion), but in presence of the energetic particles, such as ions and electrons, striking the solid surface producing secondary-electron emission (SEE).

From the theoretical point of view the present work has brought contribution to an integrated model of plasma-wall interaction with a realistic description of the plasma-wall transition, space charge sheath and presheath near the walls.

From the experimental point of view device has been realised for data concerning secondary-electron emission at the both probe and wall chamber surface in real conditions due to presence of the working gas. Data for the plasma parameters using electrical probes such as Langmuir probes and Katzumata probe and ball-pen probe in CASTOR device have been performed. New model has been proposed for Katzumata probe taking into account collisions and diffusion process across magnetic field line.

2. Results

2.1 Plasma with fast electrons and secondary electrons emitted at the probe surface

2.1.1 The case of a stationary plasma [1]

Pre-sheath analysis

We developed an analytical model and performed 1d3v PIC (one spatial and three velocity dimensions Particle-In-Cell) simulations for the Volt-Ampère characteristic of a plane electrode (wall or probe) immersed in collisional un-magnetised Deuterium plasma, where fast electrons are present. It was analysed with priority the case of negatively bias of the electrode with respect to the plasma potential when in its front a positive sheath region is formed. The ion sheath is connected with the bulk plasma by a pre-sheath region. The probe surface is perfectly absorbing with respect to the incoming particles and emits secondary electrons due to the impact of the fast electrons.

In our analytical model, inside the pre-sheath region, the electrons are described kinetically, while the ions are treated by the fluid model. We mention here briefly only the treatment of the fast electrons, thermal electrons and ion description can be found in our former detailed work [2]. The secondary electrons are considered to be cold inside the sheath and pre-sheath regions, thus their flux is assumed to be constant.

At the collisional pre-sheath entrance (CPE) the fast electrons have a shifted cut-off distribution function given by

$$f_{en}^{f}(x,v) = A_{en}^{f}\left\{\exp\left[-\left(-\sqrt{v^2 - 2e\phi(x)/m_e} + v_{sh}\right)^2 / \left(\sqrt{2}v_{et}^{f}\right)^2\right] H(-v)\right.$$
$$\left. + \exp\left[-\left(\sqrt{v^2 - 2e\phi(x)/m_e} - v_{sh}\right)^2 / \left(\sqrt{2}v_{et}^{f}\right)^2\right] H(v) H\left(v_c - v\right),\right.$$

where v_{sh} and v_{et}^{f} are the shift velocity of the beam and the thermal velocity of the fast electrons, respectively; v_c is the cut-off velocity and $\phi(x)$ represents the potential at any position x; A_{en}^{f} is a constant given by

$$A_{en}^{f} = \sqrt{2}n_{e0}^{f}\left\{\sqrt{\pi}v_{et}^{f}\left[1 + 2\,\mathrm{erf}\sqrt{\frac{E_{sh}}{kT_{pl}^{f}}} + \mathrm{erf}\left(\sqrt{-\frac{eV_p}{kT_{pl}^{f}}} - \sqrt{\frac{E_{sh}}{kT_{pl}^{f}}}\right)\right]\right\}^{-1}.$$

Here n_{e0}^{f} and T_{pl}^{f} represent the density and the temperature of the fast electrons at the CPE, respectively. We have done progresses in the analytical description of the fast electron flux inside pre-sheath region. We apply a Taylor expansion, along the pre-sheath region for the fast electron distribution function and obtain:

$$f_{en}^{f}(x,v) = A\left\{\left[1 - \chi\left(1 + \frac{v_{sh}}{v}\right)\right]\exp\left[-\left(\frac{v + v_{sh}}{v_{et}^{f}\sqrt{2}}\right)^2\right] H(-v) + \left[1 - \chi\left(1 - \frac{v_{sh}}{v}\right)\right]\right.$$
$$\left. \times \exp\left[-\left(\frac{v - v_{sh}}{v_{et}^{f}\sqrt{2}}\right)^2\right] H(v) H\left(v_c^{f} - v\right)\right\}.$$

After some simple calculations the fast-electron flux at the sheath entrance (SE) can be written as

$$\Gamma^{f}_{enSE}(x_{SE}) = A^{f}_{en}\left(v^{f}_{et}\right)^2\sqrt{\pi}\left\{\frac{1}{\sqrt{\pi}}(1-\chi_{SE})\exp\left[-\left(\sqrt{-\chi_{SE}-\frac{eV_p}{kT^{f}_{pl}}}-\sqrt{\frac{E_{sh}}{kT^{f}_{pl}}}\right)^2\right]\right.$$

$$\left.+\sqrt{\frac{E_{sh}}{kT^{f}_{pl}}}\left[1-\mathrm{erf}\left(\sqrt{-\chi_{SE}-\frac{eV_p}{kT^{f}_{pl}}}-\sqrt{\frac{E_{sh}}{kT^{f}_{pl}}}\right)\right]\right\},$$

with χ_{SE} the normalized potential value at the SE, E_{sh} the shifted energy of the fast electrons at CPE.

We demonstrate that this model allows us to estimate the secondary-electron emission coefficient of the plane-probe material. For sufficiently high secondary electron emission (SEE), the probe characteristic shows an interesting feature in that it contains three floating-potential values. By this model we approximated well the behaviour of the simulated Volt–Ampère characteristic for a fast/ion density ratio $\alpha_1 = n_{f0} / n_i = 3.98\times10^{-4}$ (see Figure1).

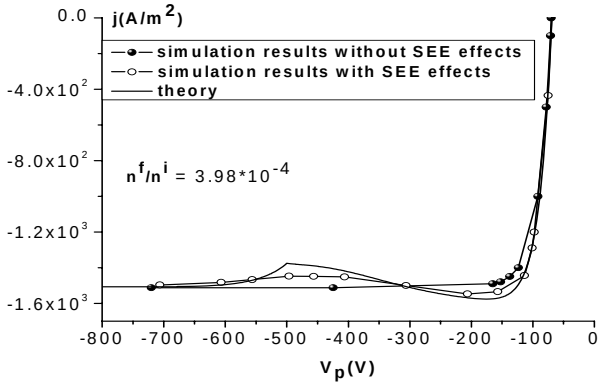

Figure 1. Volt-Ampère characteristic (magnification for negative probe biases), simulation and theory

2.1.2 The case of a turbulent plasma

We continued the study of the plasma wall transition (PWT) in presence of fast electrons, performing 1d3v PIC simulations for the Volt-Ampère characteristic of a plane probe immersed in collisional un-magnetised Deuterium plasma. The simulations were carried for a ratio of the fast electron density with respect to the ion density $\alpha_2 = n_{f0} / n_i = 1.225\times10^{-2}$.

For the stationary case of the PWT (the case of a density ratio $\alpha_1 = n_{f0} / n_i = 3.98\times10^{-4}$), the stability of the sheath and pre-sheath was analysed applying the linear perturbation method and found that the pre-sheath can not shield the probe effects further on the unperturbed plasma, the secondary electron emission (SEE) instability being not dumped into the plasma [3].

We observe now in our PIC simulation results, that an increase by two order of magnitude of the density ratio (the density ratio α_2) lead to vortex structures and the plasma of the pre-sheath is turbulent. The probe surface is perfectly absorbing with respect to the incoming particles and emits secondary electrons due to the impact of the fast electrons. Thermal electrons and ions are injected at the pre-sheath entrance (PE) with half Maxwellian

distribution function, while the fast electrons have a shifted Maxwellian distribution function. At the probe surface the secondary electrons are emitted with half Maxwellian distribution function. As is our previous report, it is analysed the case of negatively probe bias with respect to the plasma potential, when in front of the probe a positive sheath region is formed, connected with the bulk plasma by a pre-sheath region.

The simulated Volt–Ampère characteristic for the density ratio α_2 is presented in Figure 2. One can observe that the modification of the plane probe characteristic [2] induced by the fast and secondary electrons does not show three inflection points (as we have obtained for a density ratio α_1), but contrarily the total probe current is monotonically increasing by the decrease of the probe negativity.

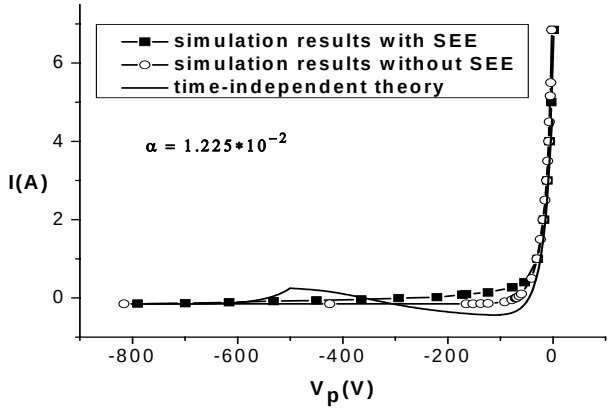

Figure 2. Current-voltage characteristics of a plane probe simulated for turbulent plasma with SEE (square symbol) and stationary plasma without SEE (circle symbol), compared with an analytical time-independent model (line)

The time-independent theory from the section A [1] gives strong errors for this case (the black curve in Figure 2). It means that we should refer to the chaotic systems that imply non-linear modifications of plasma parameters on the PWT region studied. We are now in course of elaboration of a proper analytical model to explain the behaviour of the Volt-Ampère characteristic for this kind of turbulent plasma.

2.2 Bayesian Belief Networks for enhanced collision algorithms

Collision processes have to be considered in describing ion sheath formation and properties in front of an electrode placed in magnetised hydrogen plasma. A new approach of these processes is proposed using the Bayesian Belief Network (BBN) or Bayesian Net. The BBN is a statistical theory that can be applied on a very large number of topics ranging from social studies to biology, physics and others. The application of the theory to specific problems is not a trivial task but once implemented can bring multiple benefits. The advantage of the theory is that it can deal with a large number of parameters divided in tree main categories namely hypothesis, events and conditional means or restrictions [4,5]. The main drawback is the large computational time necessary to apply this kind of method. This can be compensated by using a number of approximations and clever algorithm design.

2.2.1 Bayesian Theory. Short description

The Bayesian Theory is constructed around a simple formula that describes the probability of an event taking into consideration that another events has a specified probability that is known.

Let us consider that we have two events denoted by A (the hypothesis) and B (the evidence). The probability of the event A taking into consideration that B happened is:

$$P(A \mid B) = \frac{P(B \mid A) \cdot P(A)}{P(B)}$$

where P (A|B) is the probability of A given B, P(B|A) is the probability of B given A and it is called the likelihood. P(A) and P(B) are the probabilities of A and B regardless of any other event. $P(\cdot)$ it is referred as the prior distribution and P(A|B) is the posterior distribution.

On a given problem it can happen that we may have also conditional means or short conditions restricting the hypothesis or the events. In this case the probability of A given B taking in consideration that we are restricted by I is:

$$P(A \mid BI) = \frac{P(B \mid AI) \cdot P(A \mid I)}{P(B \mid I)}.$$

Usually the hypothesis is a set of random values but it can be also statements or just states of a system (for example the aggregation state of a system) and they are unknown quantities. In order to fully define a Bayesian Net for a given set as described above it is necessary to define the prior distributions P(A) and P(B) [4]. The selection of this distribution is strongly dependent on the studied phenomenon. There are cases in witch the selection of the prior distribution is not important because we can provide a large number of evidence for a given hypothesis and in the end the prior distribution will be lost in the computation, the system will select naturally the distribution that it needs and in principal closer to the real distributions [5].

2.2.2 Collision treatment using BBN

At this stage the collisions of particles usually are treated in a simplified manner. As input parameters we define the species that participate in a collision, the collision cross section for each species knowing the kinetic energies. Also it is defined a total collision cross section for all the collision processes used in so called null collision algorithms implemented in Monte Carlo codes. A probability of collision process is computed given the time of flight of a particle. The maximum probability of a collision event is given by the total collision cross section.

The Monte Carlo algorithm proceeds by generating a random number. If the random number is larger then the total collision probability then the particle will not collide. If the random number is lower then it is generated a second random number to decide which kind of collision the particle will suffer.

The Bayesian statistical approach can describe more accurately a collision event by differentiating between particle species, energy of projectile and target, direction of the velocity vectors or maybe internal energy of a colliding molecule (in case of simulations that

deal with complex gases). By taking in consideration a large number of input values the BBN algorithms can predict with accuracy the type of collision that will take place and, if necessary, can predict also the results of the collision.

In order to describe and construct a Bayesian Net for the collision processes we will have to specify the hypothesis, in our case the possible collision types (elastic, ionisation, excitation etc.). The role of evidence can be played by the energy of particles, the direction of the velocity vector, the charge of the particles or the presence of a third particle in the collision process. The role of the conditional means can be played for example by the particle density as a localised value (and not as an average over the hole system).

The implementation of a Bayesian statistical theory is not trivial as already mentioned, at this type of system and one should research extensively the advantages and disadvantages of such an algorithm on a given problem. It is possible that the method is too expensive in terms of computational time. In this case a number of approximations must be taken into consideration.

2.3 Experimental study of the secondary electron emission induced by electron bombardment

The emission of the secondary electrons is studied using a Langmuir plane-probe. The process is induced at the probe surface by a mono-kinetic electron beam, produced by an electron gun. The probe and the electron gun are immersed in a low temperature plasma of a multipolar confined system (similar with a DP machine, but with only one chamber). A DC discharge is produced in helium for a pressure of 10^{-4} to 10^{-3} mtorr, in a nonmagnetic stainless-steel vessel (32 cm in diameter and 40 cm in length).

The electronic gun was designed and realised in this period. The electrons are thermo-emitted by a heated filament. They are accelerated and extracted due to the negative voltage applied on the filament with respect of a metallic grid. The accelerating potential is of the order of hundreds Volts. The electrons leave the gun as a monokinetic beam. The beam is directed perpendicularly to the probe surface.

Also, we have started to design a high-voltage amplifier for probe polarisation. The high-voltage amplifier multiplies the saw-tooth signal generated by a data acquisition system up to +/- 430V. This high-voltage signal is applied on the probe as polarisation potential. Using the same data acquisition system, the current-voltage characteristic of the probe can be obtained in the presence of secondary electron emission at the probe surface.

2.4 Numerical modelling of hydrogen magnetised discharge

In order to consider the secondary electron emission produced by ion bombardment in the presence of a magnetic field, the process at the target surface of a magnetron discharge has been proposed. In this view, the fluid model developed for the description of an argon magnetron discharge [6] was considered in order to be applied to hydrogen magnetised plasma. This period was dedicated to the bibliographical research concerning the input necessary data for hydrogen. First of all there were identified the main collision processes that may occur. The corresponding elementary cross sections were processed. For electron-hydrogen interaction

we have studied ionisation, rotational excitation, vibrational excitation, dissociative excitation, elastic momentum-transfer, etc. For hydrogen heavy particles we have studied the binary interactions for the following species: H, H_2, H^+, H_2^+, H_3^+, H^-.

2.5 On the secondary electron emission in DC magnetron discharge (short description of the fluid model used for argon)

The presence of a curved magnetic field in the vicinity of a surface can drastically influence the secondary electron emission induced by ion impact. This phenomenon was studied for the metallic cathode of a DC planar magnetron discharge. The spatial dependence of the secondary electron emission coefficient is obtained from the boundary conditions imposed for particle fluxes in two-dimensional fluid model [7]. The effect of the magnetic field strength (magnitude and orientation) and electron reflection on the surface upon the coefficient of the secondary electron emission is investigated.

In the case of a planar magnetron, the ions are accelerated into the cathode fall and they bombard the cathode (also known as target) extracting from the surface secondary electrons and atoms. Due to the magnetic field presence in front of the cathode, secondary electrons follow helicoidal trajectories, allowing some of them to return to the surface despite of the strong repulsive electric field. Once back, these electrons can be either reflected or captured. All reflected electrons are re-injected into the discharge while the others stay on the target. Hence, not all of the secondary electrons are important for the discharge.

The magnetron plasma is studied with a bi-component fluid model [6]. The first three moments of Boltzmann equation are solved for electrons while only the first two of the corresponding equations are considered for the positive ions. Plasma potential is given by Poisson equation.

For the case of a magnetised discharge, the momentum transfer equation for electrons is written as $\overrightarrow{\Gamma_e} = \overrightarrow{\Gamma_e^0} + \overrightarrow{\Gamma_e^1}$, where $\overrightarrow{\Gamma_e^0}$ is the classical drift-diffusion flux and $\overrightarrow{\Gamma_e^1}$ is the contribution of the magnetic field. These terms detail as:

$$\overrightarrow{\Gamma_e^0} = -\mu_e n_e \vec{E} - \nabla(D_e n_e)$$

$$\overrightarrow{\Gamma_e^1} = -\overrightarrow{\Gamma_e} \times \overrightarrow{\Omega_e} / f_{me},$$

with μ_e the electron mobility, D_e the electron diffusion coefficient, $\overrightarrow{\Omega_e} = e\vec{B}/m_e$ the angular cyclotron velocity. The electric and magnetic fields present only radial and axial components and the plasma is supposed to be axially symmetric. Due to the axial symmetry, a cylindrical co-ordinate system is used.

Solving fluid equations requires some boundary conditions. For the charged particles these conditions are imposed for the fluxes. All the fluxes parallel to any electrode in the discharge are zero. In the absence of a magnetic field, the normal electron flux to the cathode is given only by the secondary electrons issued by ion impact on the surface $\Gamma_e^{0\perp} = -\gamma_i \Gamma_i^{\perp}$, with γ_i the coefficient of the secondary electron emission and $\Gamma_i^{\perp}$ the normal ion

flux incident to the cathode. If a magnetic field is present, the cathode boundary condition changes in $\Gamma_e^{\perp} = \Gamma_e^{0\perp} + \Gamma_e^{1\perp}$. Performing some simple calculations we obtain

$$\Gamma_e^{\perp} = -\gamma_i \Gamma_i^{\perp} \left(1 - \frac{\Omega_{e\parallel}^2}{f_{me}^2 + \Omega_e^2} \right) \equiv -\gamma_{net} \Gamma_i^{\perp},$$

with f_{me} – the total momentum transfer frequency for electron – neutral collision. The influence of the magnetic field on the ion flux is neglected because the ion cyclotron giro-radius, which is the order of several cm, is much larger than the thickness of the cathode fall, limited at a few mm. A new coefficient was introduced, γ_{net},

$$\gamma_{net} = \gamma_i \left(1 - \frac{\Omega_{e\parallel}^2}{f_{me}^2 + \Omega_e^2} \right).$$

While γ_i is a measure of all secondary electrons emitted by ion bombardment of the cathode, γ_{net} is an effective coefficient corresponding only to those secondary electrons which remain in the discharge, excluding the electrons recaptured by the cathode. The last relation reveals the dependence of γ_{net} on some discharge parameters. The total momentum transfer frequency for electron – neutral collision f_{me} depends on the gas nature and pressure, while angular cyclotron velocity vector $\overrightarrow{\Omega_e}$ contains the dependence on the magnetic field strength. The difference between the net coefficient, γ_{net}, and the ion induced one, γ_i, can be expected to vanish with the increase of the pressure due to electron-neutral collisions and also if the magnetic field lines become perpendicular to the surface.

It is noteworthy mentioning that the possible reflection of the electrons to the cathode is not included. If a non-zero reflection coefficient (R) is considered, it must be applied only to the returned electrons and the effective coefficient γ_{net} becomes

$$\gamma_{net} = \gamma_i \left[1 - \frac{\Omega_{e\parallel}^2}{f_{me}^2 + \Omega_e^2} (1 - R) \right].$$

For illustration, some typical results are presented for Argon discharge. The cathode is a metallic disc (r_{cath} = 16.5 mm). The magnetic field strength varies radially both in magnitude and direction. At the cathode surface, at $r \approx 9.5$ mm, the magnetic field strength is about 750 Gauss and it is parallel to the surface. On the discharge axis and at $r \approx 15$ mm the magnetic field lines are normal to the cathode.

In Figure 3, the net coefficient of the secondary electron emission γ_{net}/γ_i and the electron flux at the cathode $\Gamma_e^{\perp}$ are plotted for two different electron reflection coefficients (R = 0, 0.5), keeping constant the incident ion flux, $\Gamma_i^{\perp}$. The maximum ion flux corresponds to the maximum plasma density, which is confined by the magnetic field in the region where B is parallel to the cathode ($r \approx 9.5$ mm). Both fluxes in the Figure are normalised to the peak value.

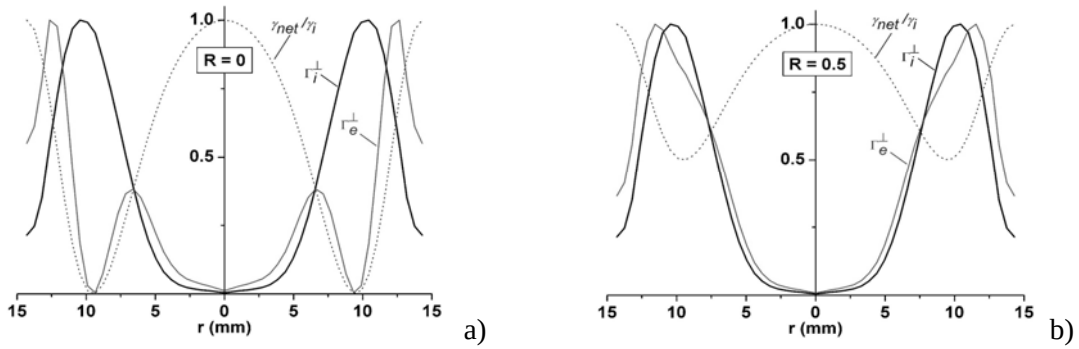

Figure 3. Radial dependence of the ratio γ_{net}/γ_i, normalised ion ($\Gamma_i^\perp$) and electron ($\Gamma_e^\perp$) fluxes at the cathode: a) R = 0; b) R = 0.5

The magnetic field inhomogeneity determines the spatial variation of the net coefficient of the secondary electron emission, with a minimum value in the region where the magnetic field lines are parallel to the cathode. This fact has an immediate influence on the flux of the secondary electrons. The minimum value of γ_{net} is controlled by the reflection probability of the electrons on the surface.

2.6 Experimental measurements on Castor Tokamak in Prague

In the period 3-11 November 2005, Prof. Dr. Gheorghe POPA and Dr. Claudiu COSTIN have directly participated to the measurements realised on Castor Tokamak, Institute of Plasma Physics, Prague, Czech Republic. There were performed measurements of the floating potential in the edge of the plasma torus, using 3 Katsumata Type probes (3KT), of 1, 2 and 4 mm in diameter each, located on the same magnetic surface or on the same magnetic field line. These probes are similar with the ball-pen probe, except that the head is flat instead of conical. All the probes are fixed on the same boron nitride plate. It is supposed that the floating potential measured with these probes is equal with the plasma potential. In the same time, for comparison, another probe of 2 mm in diameter was used to measure the floating potential, acting either as Langmuir probe or ball-pen probe. The last probe was inserted in the tokamak chamber diametrically opposite with respect of 3KT. All the probes were inserted from the top of the torus, with the possibility of being moved along the small radius of the torus. The measurements were performed to obtain the radial profile of the edge-plasma parameters. Our team contribution at this campaign was the post acquisition data processing concerning the potential measurements.

The results obtained showed that not all 3KT probes measure the same potential, as expected from the actual theory. There are two possibilities to explain the results: 1) the floating potential measured by the probes depends on the probe diameter; 2) plasma parameters vary spatially in the poloidal direction in the region where 3KT are inserted (non-homogeneous plasma).

There were also analysed the fluctuations of the floating potential measured with 3KT and the single ball-pen probe in order to get some information about plasma turbulence. A power spectrum plotted for these fluctuations showed that the amplitude of the signal decreases on increasing the frequency. Starting from this result, Prof. POPA proposed to plot first a voltage-position characteristic for the ball-pen probe and after that to investigate

the power spectrum of the floating potential fluctuations. The results show that more the probe is withdrawn in the boron nitride tube, more the high frequencies are cut. The amplitude of the signal decays exponentially with the position in the boron nitride tube. This comportment is specific for a diffusion process of the plasma inside the boron nitride tube. This hypothesis must be verified and if it will be validated the actual theory of the ball-pen probe must be reconsidered.

These results have changed the next step of the experimental part of the project as would be presented in the following.

2.7 The double probe system

The preliminary results obtained at Castor Tokamak revealed the fact that it is very difficult to use such a system as we initially intended: one probe perpendicular to the magnetic field lines and the other at a certain known angle. The main inconvenient is the lack of knowledge regarding the precise orientation of the magnetic field lines. For that, it is very difficult to know how to position the two probes. Even more, if we intend to place the two probes on the same magnetic filed line, we cannot avoid the shadow effect from one probe to the other. If we intend to place the two probes on the same magnetic surface, than it is very probable that plasma parameters vary from one probe to the other, due to the strong non-homogeneity of such plasmas.

As a consequence, we have changed the plan to design an ion analyser proposed by Prof. G. POPA, which will permit to obtain the energetic distribution of the ions, perpendicularly on the magnetic field. The principle scheme of the analyser is attached to this report. The analyser has to be positioned perpendicularly on the magnetic field lines. It is composed from a stainless steel rectangular plate (9×4×2 mm), in which are drilled 3 channels of different diameters: 0.4, 0.6 and 0.8 mm. The role of the channels is to select the ions as function of their energy, in the normal direction to the magnetic field. There is a close relation between the channel diameter and the Larmor radius of the ions that pass through the channel. Behind every channel is fixed a tungsten or stainless steel wire of the same diameter as the channel, in order to collect the passing ions. The wires are fixed in another stainless steel plate, but insulated from that with ceramic tubes. The analyser will be manufactured till the end of 2005. The first measurements are foreseen for the beginning of 2006.

The double probe system has to be used for plasma diagnostic in Magnum PSI machine. In this device the direction of the magnetic field is well known (parallel with the symmetry axis). Thus, the position of the two probes with respect of the magnetic field lines can be easily determined. According to results of the short visit made at Magnum, in July, by Prof. Dr. G. Popa and exchange of messages with Prof. Dr. Goedheer leader of Magnum project and Dr. Koppers it was decided that detailed program for collaboration concerning experiment and simulation will be fixed with beginning of 2006.

2.8 Numerical modelling of the ion analyser

The decision of using an ion analyser instead of a double probe system has also changed the modelling projects. For preliminary results, we propose a simplified numerical

model for the ion analyser, permitting to deduce the fraction of the ions that can be collected as a function of the aperture diameter of the analyser channels. In the first step, only one channel will be studied, via PIC simulation. Once the results obtained for one channel, the diameter can be modified, providing thus results for all channels.

As already mentioned, the magnetic field lines are perpendicular on the analyser, in other words, parallel with the channel axis. The ions will be introduced in the channel at random radial position, with random velocity direction and with a maxwellian velocity distribution function in the perpendicular plane on the magnetic field lines. Along the field lines, the ion velocity can be mono-kinetic or maxwellian distributed. The motion equation will be integrated for every ion and we will count if the ion pass through the channel or is collected by the channel wall. After a statistical calculus, we can provide information about the ratio between the ions that pass through the channel and the lost ones at the channel wall, correlated with the ion energy normal to the magnetic field.

If we consider only the geometrical ratio between the ion Larmor radius and the channel diameter, at the exit of the channel will arrive at the most those ions having the specified ratio smaller than 0.5. The first plate of the analyser will collect the others. The critical Larmor radius that separates the two ion categories corresponds to a critical value of the ion energy perpendicular on the magnetic field lines, $\varepsilon_i^{\perp}$. An estimation of this specific energy is shown in the table 1 for atomic hydrogen ions in a magnetic field of 1T.

Table 1. Correlation between channel diameter, critical Larmor radius and critical ion energy

Channel diameter (mm)	H ion radius (mm)	$\varepsilon_i^{\perp}$ (eV)
0.4	0.2	2
0.6	0.3	4.45
0.8	0.4	8

The data in the table 1 show that the channel of 0.4 mm in diameter can be passed through by the ions with a maximum energy perpendicular on the magnetic field lines of 2 eV and so on. In reality, not only the ratio between the ion Larmor radius and the channel diameter is important. But, also the energy distribution of the ions along the field lines comparing with the ion energy distribution perpendicular to the field lines plays a role because of the finite ration between length and diameter of the channel. We expect that the simulations in this direction will provide more accurate results.

3. Conclusions

Regarding the theoretical and numerical approaches, we have realised the objectives proposed for the year 2005, our contribution being related especially to the plasma wall transition in magnetised regions, focusing on the secondary electron emission on the surface.

Concerning the experiments, the measurements made in Castor Tokamak with Katsumata type probes determined us to change the tools dedicated for magnetised plasma diagnostic, replacing thus the double probe system with a multi-channel ion analyser. The double probe system remains as a possibility of plasma diagnostic in Magnum-Psi device.

All the research directions started in 2005 will continue in 2006 in order to complete the results that were already obtained.

4. Expected results for 2006

Test results of the measurements performed in the edge plasma of CASTOR Tokamak with the multi-channel analyser designed to deliver information about ion energy distribution perpendicularly on the magnetic field.

Results concerning diffusion model for Katsumata type probe from the measurements for plasma potential fluctuations in the edge plasma of CASTOR Tokamak.

An analytical and numerical model for Katsumata type probe.

Experimental results regarding the secondary electron emission at the probe (and wall) surface in a multipolar confinement system.

Collisions implementation in a non-collisional model for the description of the sheath formation in front of a conductive wall.

An analytical and numerical model for the ion multi-channel analyser.

References

[1] **Teodoru S., Kuhn S., Tskhakaya D. jr. and Popa G.,** "*Time-independent theory and simulation results for a collisional plasma-wall-transition (PWT) in presence of fast electrons*", the 4th International Conference on Global Research and Education, Wuppertal, Germany, 19–22 September 2005

[2] **Teodoru S., Tskhakaya D. jr., Kuhn S., Tskhakaya D. D., Schrittwieser R., Ionita C. and Popa G.,** "*Kinetic (PIC) simulation for a plane probe in a collisional plasma*", J. Nucl. Mat. 337 (2005) 168

[3] **Teodoru S., Kuhn S., Tskhakaya D. jr. and Popa G.,** "*Is the plasma at a plane probe unstable in the presence of fast electrons producing secondary electrons?*", the 32nd EPS Conference of Plasma Physics, Tarragona, Spain, 27 June-1 July 2005

[4] **Geweke J. and Tonizaki H.**, "*Bayesian estimation of state-space models using the Metropolis-Hastings algorithm within Gibbs sampling*", Computational Statistics & Data Analysis 37 (2001) 151

[5] **Breese J. and Koller D.**, "*Bayesian Networks and Decision-Theoretic Reasoning for Artificial Intelligence*", September 1997, http://ai.stanford.edu/~koller/BNtut/

[6] **Costin C., Marques L., Popa G. and Gousset G.**, *"Two-dimensional fluid approach to the DC magnetron discharge*", Plasma Sources Sci. Technol. 14 (2005) 168

[7] **Costin C., Popa G. and Gousset G.,** "*On the secondary electron emission in DC magnetron discharge*", Journal of Optoelectronics and Advanced Materials 7 (2005) 2465

Collaborative actions

Measurements realised at the Institute of Plasma Physics, Prague, Czech Republic, in collaboration with Association EURATOM/ IPP.CR, concerning probe measurements in the edge region of Castor Tokamak and numerical modelling of the type of probes used in experiments. This collaboration will continue in 2006, on the same two directions, measurements and modelling. To the campaign realised in Prague have also participated the researchers from Institute for Ion Physics and Applied Physics, University of Innsbruck, Austria, Association EURATOM/ ÖAW and from Consorzio RFX, Padova, Italy, Association EURATOM/ ENEA.

Collaboration with the Institute for Theoretical Physics, University of Innsbruck, Austria, Association EURATOM/ ÖAW, regarding the numerical modelling of plasma-wall interaction, for plasmas with fast electrons and secondary electrons emitted at the wall surface.

Dr. V. Pericoli from ENEA, Frascati, Italy, Association EURATOM/ ENEA, has made a visit in our institution in the perspective of a future collaboration in 2006 regarding measurements using a multi-channel ion analyser.

Prof. Dr. G. Popa has made in 2005 a short visit at FOM Institute for Plasma Physics "Rijnhuizen", Holland, Association EURATOM/ FOM. It was decided that detailed program for collaboration concerning experiments and simulations for Magnum-Psi device will be fixed starting with the beginning of 2006.

In October 2005, our institution was the hostess and one of the organisers of the exhibition Fusion Expo in Romania.